The Egyptian Journal of Radiology and Nuclear Medicine 47 (2016) 1361–1372

Contents lists available at ScienceDirect

The Egyptian Journal of Radiology and Nuclear Medicine

journal homepage: www.sciencedirect.com/locate/ejrnm

Original Article

Multi-phasic CT versus dynamic contrast enhanced MRI in characterization of parotid gland tumors

Mohamed Metwally Abo El Atta, Talal Ahmed Amer, Ghada Mohamed Gaballa, Nehal Tharwat Mohammed El-Sayed *

Department of Radiodiagnosis and Interventional Radiology, Faculty of Medicine, Mansoura University, Egypt

ARTICLE INFO

Article history:
Received 12 May 2016
Accepted 19 July 2016
Available online 24 August 2016

Keywords:
Dynamic contrast enhanced MRI (DCE-MRI)
Multiphasic CT
Parotid gland tumors

ABSTRACT

Objective: Salivary gland tumors are challenging as regards preoperative diagnosis. The aim of our study was to highlight the value of multiphasic CT and contrast enhanced dynamic MRI in characterization of benign and malignant parotid tumors as well as to compare diagnostic accuracy of both modalities.

Patients and methods: Study group included 45 patients (54 lesions), 26 males and 19 females, their age ranged from 24 to 78 years. All patients underwent both CT and MRI examinations. Time intensity (or attenuation) curve for each lesion is analyzed and compared with the final post-operative pathology.

Results: Type of the curve on dynamic contrast enhanced MRI had high sensitivity, specificity, positive predictive, negative predictive values and accuracy in characterization of benign and malignant parotid tumors (94.4%, 97.2%, 94.4%, 97.2%, and 96.3% respectively). Also, curve analysis on multiphasic CT revealed similar high sensitivity, specificity, positive predictive, negative predictive values and accuracy as compared to DCE-MRI (92.6%, 96.3%, 92.6%, 96.3%, and 95.1% respectively).

Conclusion: Both dynamic contrast enhanced MRI and multiphasic CT have comparable high accuracy in characterizing the different histological types of parotid gland tumors.

1. Introduction

Salivary gland tumors represent about 3% of head and neck tumors. Approximately 70% of salivary gland tumors occur in the parotid gland [1,2]. It is of great importance to differentiate between benign and malignant tumors for optimal surgical planning as superficial parotidectomy is performed for benign tumors. On the other hand, total parotidectomy with or without sacrifice of the facial nerve branches is performed for malignant tumors [3].

Diagnosing malignant parotid tumors based on clinical findings has its own limitations. Few symptoms, such as facial palsy, predict malignancy. Mostly, both benign and malignant parotid gland tumors grow slowly. So, preoperative radiologic assessment plays the main role in surgical planning by accurate determination of the nature and the location of the tumor [4].

Parotid gland exhibits different histologic types and subtypes of primary tumors. So, the management of its tumors requires understanding of anatomic details and pathology. Furthermore, appropriate surgical approach requires also the determination of histologic subtype of

Peer review under responsibility of The Egyptian Society of Radiology and Nuclear Medicine.

* Corresponding author.
E-mail address: nehaltharwat83@gmail.com (N. Tharwat Mohammed El-Sayed).

http://dx.doi.org/10.1016/j.ejrnm.2016.07.013

benign or malignant lesions. As regards Warthin tumor, the risk of local recurrence when managed by enucleation is about 2%, whereas, the risk for local recurrence is reported to be about 85% in pleomorphic adenoma managed in the same manner. Therefore, different surgical procedures are used among not only benign but also malignant tumors [5].

Ultra-sonography as an initial evaluation is particularly a valuable tool for assessing parotid gland lesions because it is cheap, easy, and widely available. Its disadvantages are; it is operator dependent, and of less value in deep parotid lobe and facial nerve evaluation [4].

Preoperative fine needle aspiration biopsy (FNAB) proved to be reliable in the diagnosis of parotid tumors. However, few lesions may be impossible to differentiate by only FNAB [6]. Also, inflammatory lesions of the parotid glands may mimic epithelial tumors at cytology because desquamated cells commonly simulate the former [7]. In addition, FNAB may be inconclusive due to deficient sample, small lesion size, or tumors of the deep parotid gland lobe [8].

Static MR imaging of parotid tumors had shown some suggestive characters; bright T2 signal and polylobulations could suggest pleomorphic adenoma, low T2 signal and cystic spaces suggest Warthin tumor, while malignant neoplasms may be suggested in the presence of high-grade tumors with infiltrative margins. However, these features alone cannot accurately characterize parotid tumors [9].

The role of static MRI in characterization of parotid gland tumors appears to be debatable, except for deep infiltration of malignant masses. Time to peak enhancement (TTP) and washout ratio (WR) obtained from time intensity curves (TICs) at DCE-MRI are very valuable in characterization of parotid gland tumors [10].

Several studies have evaluated the role of CT in differentiating parotid gland tumors [11]. As regards multiphasic CT, very few data on the percentage enhanced wash-out ratios among pleomorphic adenomas, Warthin tumors and malignant tumors have been analyzed [12].

The purpose of our study was to compare the diagnostic accuracy of multiphasic CT examination with DCE-MRI in characterization and differentiation of various histologic types of parotid tumors (pleomorphic adenoma, Warthin tumor and malignant tumors) as to our knowledge, there are no data in the literature compared between these specific imaging techniques.

2. Patients and methods

2.1. Patient population

This study was approved by our institutional review board, and informed patient consent was obtained before participation in the study according to institutional and native guidelines. This prospective study was performed between February 2013 and December 2015. Sixty-five patients were included in the study. Twenty patients were excluded from all analysis; 5 due to missed final pathological diagnosis, 8 proved to have inflammatory lesions and 7 patients underwent only one modality of examination (either CT or MRI only). The final study group included 45 patients. They were 26 males and 19 females, their age ranged from 24 to 78 years with mean age of 51.06 ± 11.48 years.

All patients (45) underwent both CT and MRI examination. All patients underwent complete clinical examination, history taking including drug administration, routine serum creatinine evaluation and preliminary ultrasound examination. The final post-operative pathology was the gold standard for diagnosis.

2.2. Multi-phasic CT technique and image analysis

CT was done by a 64 row multi-slice volume scanner 'Brilliance 64 CT scanner, Philips Healthcare, Best Netherlands' with fixed technique of examination. For early enhanced image (30 s), scanning began from skull base to the thoracic inlet. For the non-enhanced and delayed-enhanced images (90 s, 5 min), the scanning range was limited to the parotid gland in order to decrease radiation dose for the patient and not to compromise image quality. Helical CT acquisition parameters; 5-mm slice thickness, 120 kVp, 200 mA, 7.5 mm/s table speed, 0.8-s rotation time, pitch of 0.625, and 5 mm reconstruction interval in pre- and postcontrast images during which patient held their breath and stopped deglutition to obtain best image quality.

First, a non-enhanced examination of the parotid gland was done. Then 50–80 ml of non-ionic contrast material was given intravenously at a rate of 2 ml/s using a power injector. In all patients, the second, third, and fourth images were obtained 30 s, 90 s, and 5 min after the start of contrast material injection respectively. The images were obtained with standard soft tissue settings (window width 300 HU; window level 40 HU).

The images were transferred to a work-station and reviewed by the radiologist. All images were evaluated in each phase, and the mean density of the lesion was calculated in Hounsfield units using a region of interest (ROI) that includes solid portion of the tumor. A standardized ROI was used for all cases.

The ROI circle was made with adequate margin to avoid partial volume effects. Necrotic, cystic, hemorrhagic components, and calcification of the parotid gland lesions, were excluded, if they were present. Necrosis was considered as having attenuation value of water (−20 HU to 20 HU) on non-contrast enhanced CT. On the other hand, calcification is defined as a region having attenuation value more than 120 HU on non-contrast enhanced CT. Density numbers were recorded and averaged for data analysis. The CT numbers, for each lesion, in all phases were compared. A plot representing the time-attenuation curve was constructed for each lesion.

2.3. Dynamic contrast enhanced MRI technique and image analysis

The study was performed on Philips Enginia 1.5 T MRI scanner for all patients. Dedicated multichannel head and neck coil has been used. First, pre-contrast scan was

performed; then followed by intravenous administration of gadopentetate dimeglumine (GD-DTPA) (Magnevist) contrast agent. The following sequences are included in MRI examination: Axial T1-turbo spin echo (TSE) without Fat suppression, coronal T2-Turbo spin echo with fat suppression, and axial as well as coronal T2 sequence without fat suppression. Axial T1-weighted image (600/20/2) [TR/TE/number of excitations]; field of view: 18 cm; matrix: 256 × 192; section thickness: 2 mm; section gap: 1 mm) and T2-weighted image (4000/90/4); field of view: 18 cm; matrix: 256 × 256; section thickness: 2 mm; section gap: 1 mm) images were acquired before contrast administration.

A dynamic axial T1 fat suppressed fast-spoiled gradient recalled sequence (10.4/2.3/1; flip angle: 30°; field of view: 18 cm; matrix: 256 × 128; section thickness: 4 mm; section gap: 1 mm) with total acquisition time of 300 s was acquired during bolus injection (0.1 mmol/kg) of single intravenous dose of contrast agent gadopentetate dimeglumine (Magnevist) at a rate of 2.5 ml/s given via an automatic injector followed by 20 ml saline flush. Sequential images through the lesion were obtained in axial plane and at different time intervals (at 30, 60, 90, 120, 150, 180, 240 and 300 s following injection). Following dynamic acquisition, conventional postcontrast MR images are acquired in axial, sagittal and coronal planes.

Multiphase dynamic images were transferred to Philips extended work space (EWS) release 2.6 workstation and then analyzed. We placed a ROI within an area of the tumor that exhibited the greatest degree of early enhancement on the dynamic scanning, (avoiding cystic parts, necrosis, vessels, calcifications and hemorrhages). Time signal intensity curve (TIC) in the ROI of each examination was plotted. TIC parameters analyzed included TTP (time to peak enhancement) and WR (washout ratio).

According to the TIC tumor classification described by Yabuuchi et al. the parotid tumors are categorized into four TIC types (Fig. 1): type A, time to peak more than 120 s (this is considered a gradual enhancement); type B, time to peak 120 s or less, with high washout ratio (⩾30%) (this is considered early enhancement and high washout); type C, time to peak 120 s or less, with low washout ratio (<30%) (this is considered early enhancement and low washout); and type D, flat (seen in markedly cystic tumors) [13]. All MR imaging findings together with the tumor specific TIC were correlated with the final histopathologic diagnosis.

Semi quantitative and quantitative assessment of the DCE-MRI was done. Semi quantitative assessment was done using TIC. Quantitative assessment was done by measuring TTP and wash out rate values.

2.4. Statistical analysis

All data were collected, tabulated and statistically analyzed using SPSS 16.0. Continuous data are expressed as mean ± SD & median (min, max), and the categorial data are expressed as number (percentage). Continuous variables were checked for normality by using Shapiro-Wilk test. Mann-Whitney U (MW) test was used to compare two groups of non-normally distributed data and independent t test for normally distributed data. Percent of categorial variables were compared using the Chi-square (X^2) test and Fischer exact test. All tests were two tailed. $P < 0.05$ was considered statistically significant and $P < 0.01$ was considered highly statistically significant. $P > 0.05$ was considered non-statistically significant.

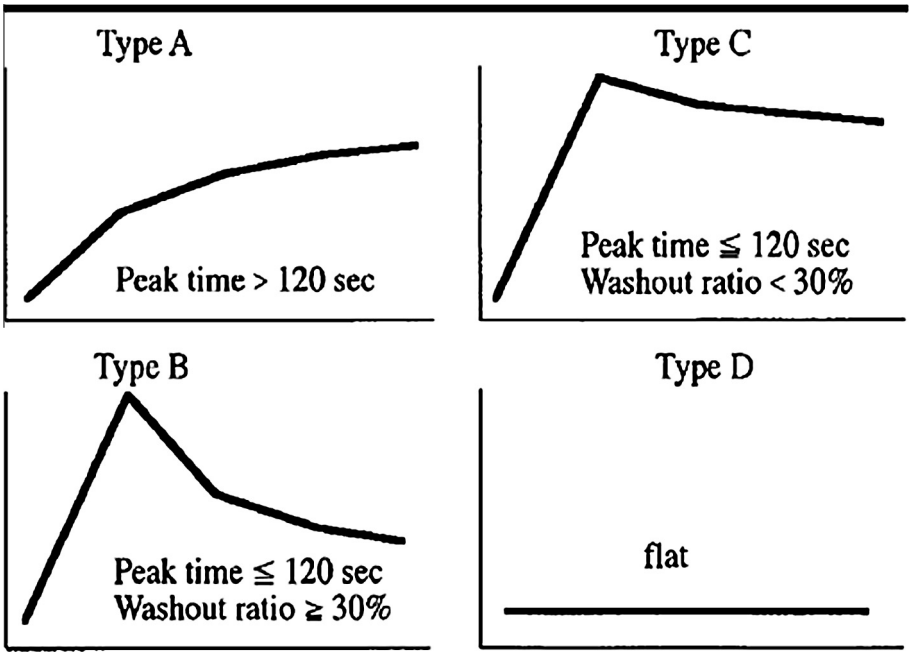

Fig. 1. TIC tumor type classifications quoted from Yabuuchi et al. [13].

3. Results

This prospective study included 45 patients having parotid gland tumors with their age ranging from 24 to 78 years with mean age of 51.06 ± 11.48 years. They were 26 males and 19 females.

Forty five patients included 19 patients with pleomorphic adenoma, 14 patients with Warthin tumors, 3 patients with muco-epidermoid carcinoma, 2 patients with acinic cell carcinoma, 2 patients with carcinoma ex pleomorphic adenoma, 3 patients with lymphoma, and 2 patients with metastatic lesions.

Forty one patients had unilateral lesions, while four patients had bilateral lesions (3 Warthin tumor and 1 lymphoma patients). Number of lesions detected in each patient ranged from 1 to 3 lesions with a median of 1 lesion. Thirty nine patients had single lesion, 3 patients had two lesions (1 Warthin tumor, 1 lymphoma, and 1 carcinoma ex pleomorphic adenoma patients) and three patients had three lesions (all were Warthin tumor patients). The total number of lesions detected was 54 lesions.

Regarding the parotid lobe involved, twenty five lesions were located in the superficial lobe, twenty seven lesions were located in both superficial and deep lobes, one lesion was located in the deep lobe and one lesion was located in a peri-parotid LN (Warthin tumor).

According to the final post-operative histopathologic reports, this study included forty benign lesions and fourteen malignant lesions.

Forty benign lesions included 19 pleomorphic adenomas, 21 Warthin tumors. Fourteen malignant lesions included 4 lymphomas, 3 muco-epidermoid carcinomas, 3 carcinoma ex pleomorphic adenomas, 2 acinic cell carcinomas, and 2 metastatic lesions.

Tables 1 and 2 demonstrate the distribution and the number of the pathologic lesions in our study with their corresponding curve type detected by multiphasic CT as well as dynamic contrast enhanced MRI study.

In our study, using type A curve on multiphasic CT as a predictor for pleomorphic adenoma had high sensitivity, specificity, positive and negative predictive values (100%, 94.3%, 90.5%, 100% respectively) (Fig. 2). Using type B curve as a predictor for Warthin tumor also had high sensitivity, specificity, positive and negative predictive values (85.7%, 100%, 100%, and 91.7% respectively) (Fig. 3). Using type C curve as a predictor for malignancy also revealed high sensitivity, specificity, positive and negative predictive values (92.9%, 95%, 86.7%, and 97.4% respectively) (Fig. 4).

On dynamic MRI, type A curve was tested as a predictor for pleomorphic adenoma, type B curve as a predictor for Warthin tumor, and type C curve as a predictor for malignancy. All revealed high sensitivity, specificity, positive and negative predictive values (100%, 94.3%, 90.5%, 100% for pleomorphic adenoma) (Fig. 2), (90.5%, 100%, 100%, 94.3% for Warthin tumor) (Fig. 3) and (92.9%, 97.5%, 92.9%, 97.5% for malignancy) (Fig. 4).

4. Discussion

Our study revealed that benign tumors are more common (representing 74%) than malignant tumors (representing 26%). These results are in agreement with a study by Salama et al. [14] who found that benign tumors were 18 (72%) while the malignant tumors were 7 (28%). Generally, pleomorphic adenoma has been regarded as the most common benign parotid gland tumor followed by Warthin tumor [9,15]. The present study showed similar results since there were 19 pleomorphic adenoma cases versus 14 Warthin tumor cases.

Here in the study, there was statistically significant difference between the age group having benign tumors (average age 48.92 ± 10.75) and those having malignant tumors (average age 57.07 ± 11.81), so malignant tumors affected older age group. This is in agreement with Salama et al. [14] who found that the mean age for benign tumors was 46.23 years while for malignant tumors was

Table 1
Multi-phasic CT time attenuation curve type detected in different parotid tumors.

Pathology	No. of lesions on CT	Type A curve	Type B curve	Type C curve
Pleomorphic adenoma	**19**	**19**	**–**	**–**
Warthin Tumor	**21**	**1**	**18**	**2**
Muco-epidermoid carcinoma	**3**	**–**	**–**	**3**
Carcinoma ex pleomorphic adenoma	**3**	**–**	**–**	**3**
Acinic cell carcinoma	**2**	**1**	**–**	**1**
Metastatic lesions	**2**	**–**	**–**	**2**
Lymphoma	**4**	**–**	**–**	**4**

Table 2
DCE-MRI time intensity curve type detected in different parotid tumor.

Pathology	No. of lesions on MRI	Type A curve	Type B curve	Type C curve
Pleomorphic adenoma	**19**	**19**	**–**	**–**
Warthin Tumor	**21**	**1**	**19**	**1**
Muco-epidermoid carcinoma	**3**	**–**	**–**	**3**
Carcinoma ex pleomorphic adenoma	**3**	**–**	**–**	**3**
Acinic cell carcinoma	**2**	**1**	**–**	**1**
Metastatic lesions	**2**	**–**	**–**	**2**
Lymphoma	**4**	**–**	**–**	**4**

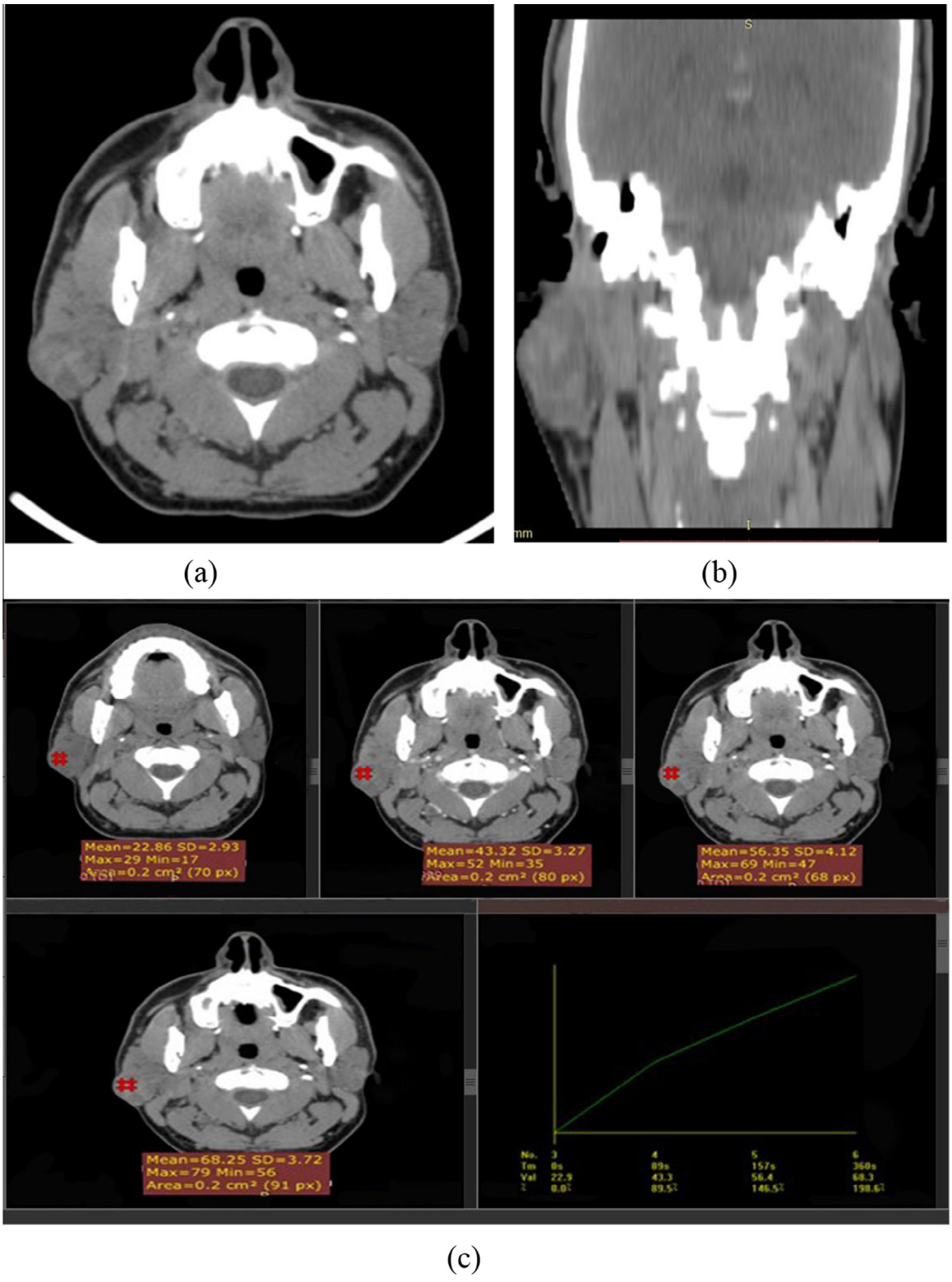

Fig. 2. A 32-years-old man with right parotid gland pleomorphic adenoma. (a and b) Axial and coronal postcontrast CT showing ill-defined heterogeneously enhancing lesion in the superficial lobe of the right parotid gland, and the lesion is separable from intra-parotid vessels. (c) Multiphasic dynamic CT with density measurement and generation of time attenuation curve revealed progressive gradual enhancement similar to type A curve detected on dynamic MRI. (d) Axial T2 weighted MRI showing that the lesion has well defined margin and high T2 SI. (e) Postcontrast MRI the lesion shows heterogeneous enhancement. (f and g) Dynamic MRI with generation of TIC revealed that the lesion has type A curve with gradual progressive enhancement and TTP 177s.

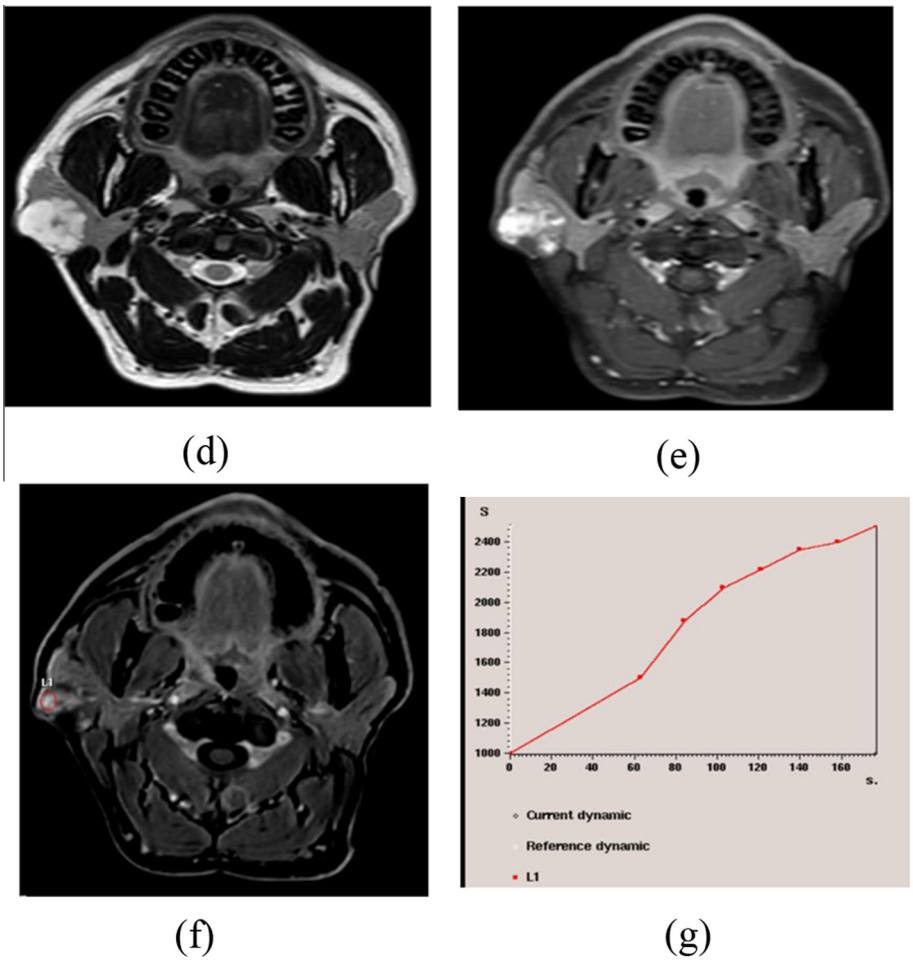

Fig. 2 (*continued*)

59.44 years. Similar results are also reported by Celebi et al. [16] who reported that the mean age was higher in malignant tumors (about 55 years) compared to benign tumors (about 45 years).

The main significant limitations of MRI are that it could not be done in patients having claustrophobia or with internal ferromagnetic device. Also, it is a relatively costly technique, long imaging time is required in some patients and lacks definition of stones and calcification. On the other hand, MRI demonstrates better soft tissue differentiation [17]. CT findings including location, size, density, bilateral occurrence, contour, intra-tumoral calcification, or multiplicity are deficient in differentiating parotid gland tumors. Previous studies indicated that the CT time attenuation curve could be valuable in the dynamic examination of parotid tumors [18].

Yerli et al. [11] and Choi et al. [18] reported that pleomorphic adenomas enhance gradually and that delayed enhancement is a powerful indicator of pleomorphic adenoma. Xu et al. [19] also found that all pleomorphic adenomas in their study were enhanced gradually, in agreement with previous reports. In the quantitative assessment, Öner et al. [20] found that tumoral mean density numbers were highest for Warthin tumors, followed by malignant tumors, and then pleomorphic adenomas in early phase scan. While tumoral mean density numbers were highest for pleomorphic adenomas, followed by malignant tumors, and then Warthin tumor in delayed phase scan. The time-attenuation curves obtained in their study were corresponding to the TICs of previous DCE-MRI studies [13].

Yerli et al. [11] reported that it is necessary to perform the CT study of a parotid tumor as soon as possible, and this is especially important with uncooperative patients. In their study 4-phase dynamic CT images were acquired at 30 s, 90 s, 5 min, and 25 min after contrast injection. However, they found that routine 25-min scanning was not practical, and it is more useful to evaluate parotid gland tumor using only 3-phase dynamic CT (i.e., possible peak enhancement time of 30 s, 90 s, and 5 min).

Our multiphasic CT study was performed by obtaining images before contrast, then 30 s, 90 s, and 5 min after contrast administration that allowed generation of time attenuation curve similar to those described by dynamic MRI. The results of our study were similar to the above mentioned ones. The study found that pleomorphic adenoma depicted gradual enhancement with peak

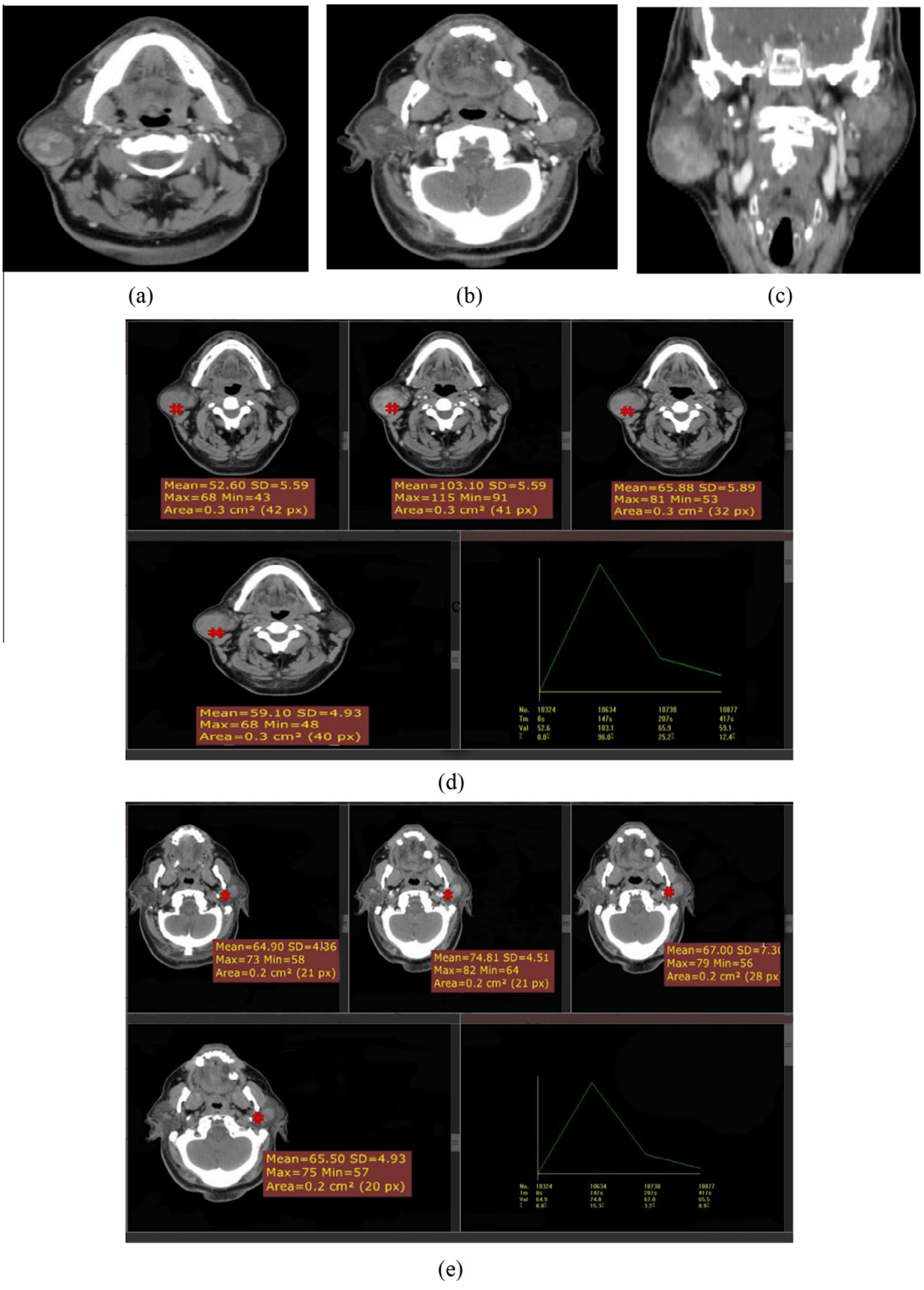

Fig. 3. A 54-years-old male patient with bilateral Warthin tumors. (a–c) Axial and coronal postcontrast CT revealed bilateral heterogeneously enhancing lesions involving superficial lobe of the right parotid and both superficial and deep lobes of the left parotid gland. (d and e) Dynamic multiphasic CT with density measurements and generation of time attenuation curve revealed that both lesions show early enhancement and rapid high washout similar to type B curve detected on MRI. (f and g) Axial T1 weighted MRI showing that both lesions have mixed low and high SI on T1 WI (notice that there is small left peri-parotid LN). (h–j) Axial and coronal T2 WI also show that both lesions have mixed SI on T2 WI. (k and l) Postcontrast MRI demonstrating that both lesions show heterogeneous enhancement. (m–p) Dynamic MRI show that both lesions have type B curve with early enhancement and rapid high washout >30%.

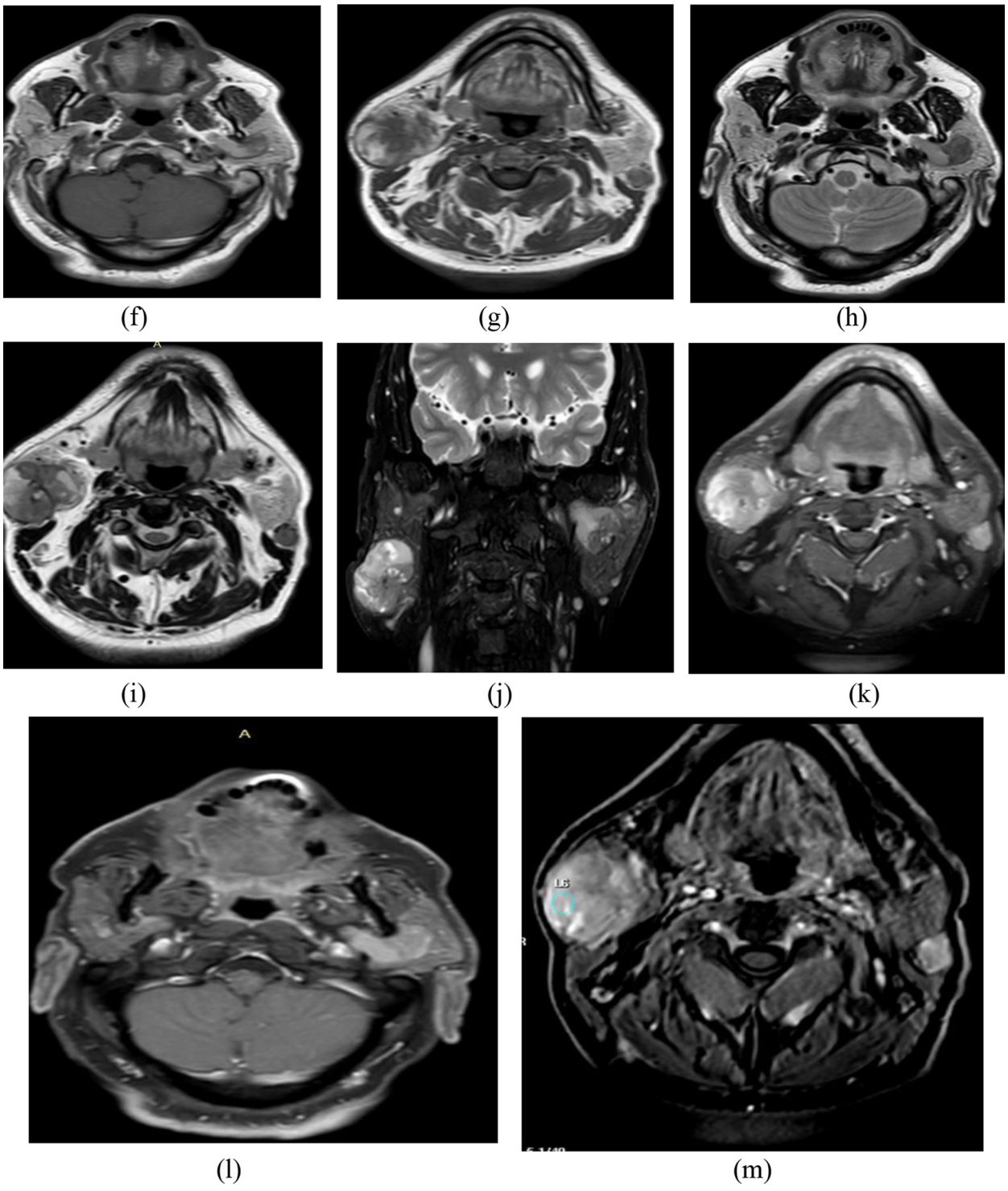

Fig. 3 (*continued*)

enhancement at the delayed phase with sensitivity, specificity, positive and negative predictive values of 100%, 94.3%, 90.5%, and 100% respectively. Warthin tumor showed rapid enhancement and high washout with sensitivity, specificity, positive and negative predictive values of 85.7%, 100%, 100%, and 91.7% respectively. Malignant

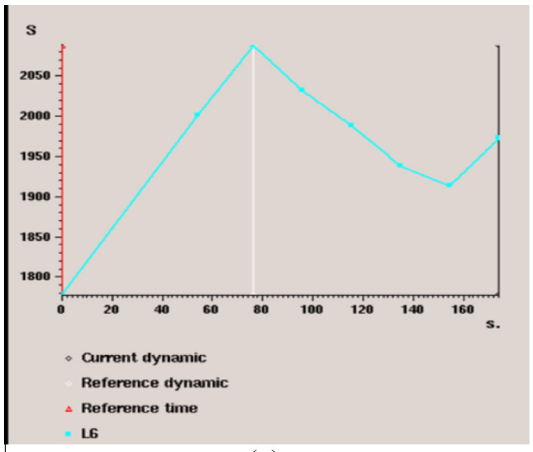

(n)

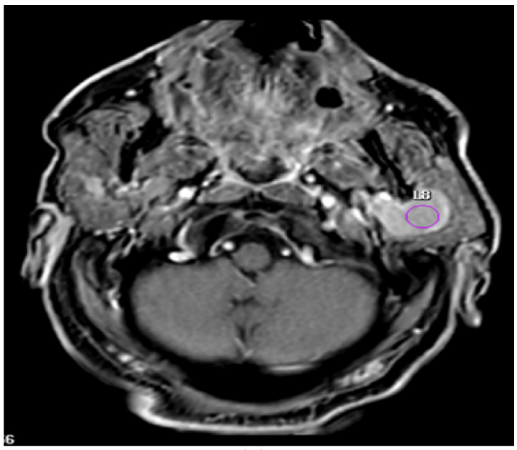

(o)

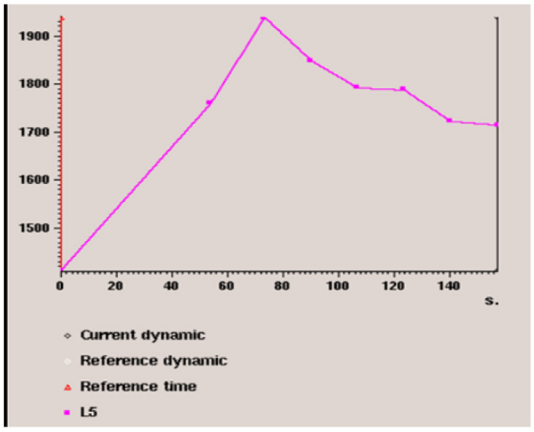

(p)

Fig. 3 (*continued*)

tumors depicted low wash out in the delayed phase with sensitivity, specificity, positive and negative predictive values of 92.9%, 95%, 86.7%, and 97.4% respectively.

Therefore time attenuation curve analysis on dynamic multiphasic CT showed high sensitivity, specificity, positive predictive, negative predictive values and accuracy in characterization of benign and malignant tumors (92.6%, 96.3%, 92.6%, 96.3%, and 95.1% respectively).

Regarding dynamic TIC we followed those described by Yabuuchi et al. [13]. They analyzed TIC parameters and found that, TTP closely correlated with micro-vessel count and the Washout ratio (WR) reflected accurately the cellularity-stromal grade. The micro-vessel count represents tumor vascularity, and thus TTP will be short when the micro-vessel count is high. The WR relies upon the difference in the amount of the contrast material between the intravascular and extravascular phases within the tumor. Large extracellular space with fibrous stroma retains the contrast material for a certain period. Thus, tumors with high cellularity-stromal grade retain less contrast and have a high WR. On the other hand, tumors with a low cellularity-stromal grade will have a low WR.

The long TTP for pleomorphic adenomas is consistent with their low micro-vessel count and low cellularity-stromal grade. The short TTP and high WR for Warthin tumors reflected their high micro-vessel count and high cellularity-stromal grade. The short TTP and low WR for malignant tumors could be explained by their high micro-vessel count and low cellularity-stromal grade [21].

According to a study by Yabuuchi et al. [13], TTP of 120 s allowed the differentiation between pleomorphic adenomas and malignant tumors. On the other hand, evaluation of the TTP alone did not allow the differentiation between Warthin tumors and malignant tumors. The WRs for malignant tumors were significantly lower than those for Warthin tumors. Therefore, the combined evaluation of TTP and WR allowed the differentiation between pleomorphic adenomas, Warthin tumors, and malignant tumors. Therefore, TIC types classified according to TTP and WR had high sensitivity and specificity in the characterization of benign and malignant tumors.

El Shahat et al. [10] reported that pleomorphic adenomas exhibited gradual enhancement pattern, (type A TIC), Warthin tumors depicted an early peak of enhancement

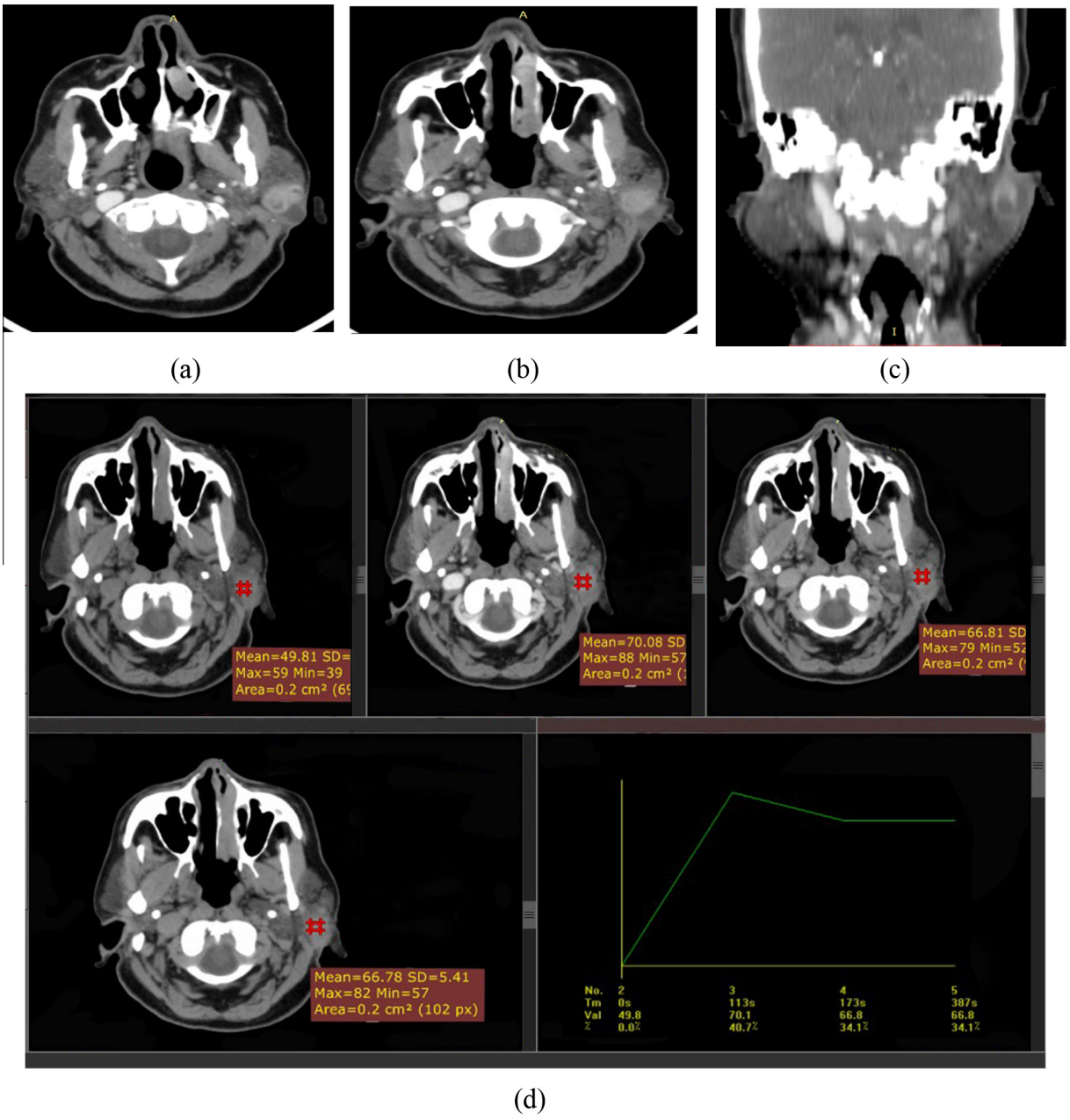

Fig. 4. A 65-years-old female patient with left parotid mucoepidermoid carcinoma (a and b) axial and (c) coronal multi-slice postcontrast CT revealed partially ill defined lesion in the superficial lobe of the left parotid gland, the lesion is partially solid and partially cystic, it is seen extending beyond the gland with infiltration of the overlying subcutaneous fat and skin. The lesion shows heterogeneous enhancement, and the lesion is separable from intraparotid vessels. (d) Dynamic multiphasic CT with density measurement and generation of time attenuation curve revealed early enhancement with low delayed washout corresponding to type C curve on dynamic MRI. (e) Shows that the lesion has low SI on T1 weighted MRI (f and g) mixed SI is noted on T2 WI. (h–j) Axial and coronal postcontrast MRI the lesion shows heterogeneous enhancement of the solid component. (k and l) Dynamic MRI revealed type C curve with TTP = 25 s and low washout <30%.

and a high washout pattern, (type B TIC), while malignant tumors depicted an early peak of enhancement and a low washout pattern, (type C TIC).

Our study revealed similar results since, type A TIC was tested as a predictor for pleomorphic adenoma, type B TIC as a predictor for Warthin tumor, and type C TIC as a predictor for malignancy. All revealed high sensitivity, specificity, positive and negative predictive values as follows: 100%, 94.3%, 90.5%, 100% for pleomorphic adenoma, 90.5%, 100%, 100%, 94.3% for Warthin tumor and 92.9%, 97.5%, 92.9%, 97.5% for malignancy.

Eissa et al. [9] tested type C curve as a predictor of malignancy against other types of TICs. But their study had a lower validation results (moderate 63% sensitivity

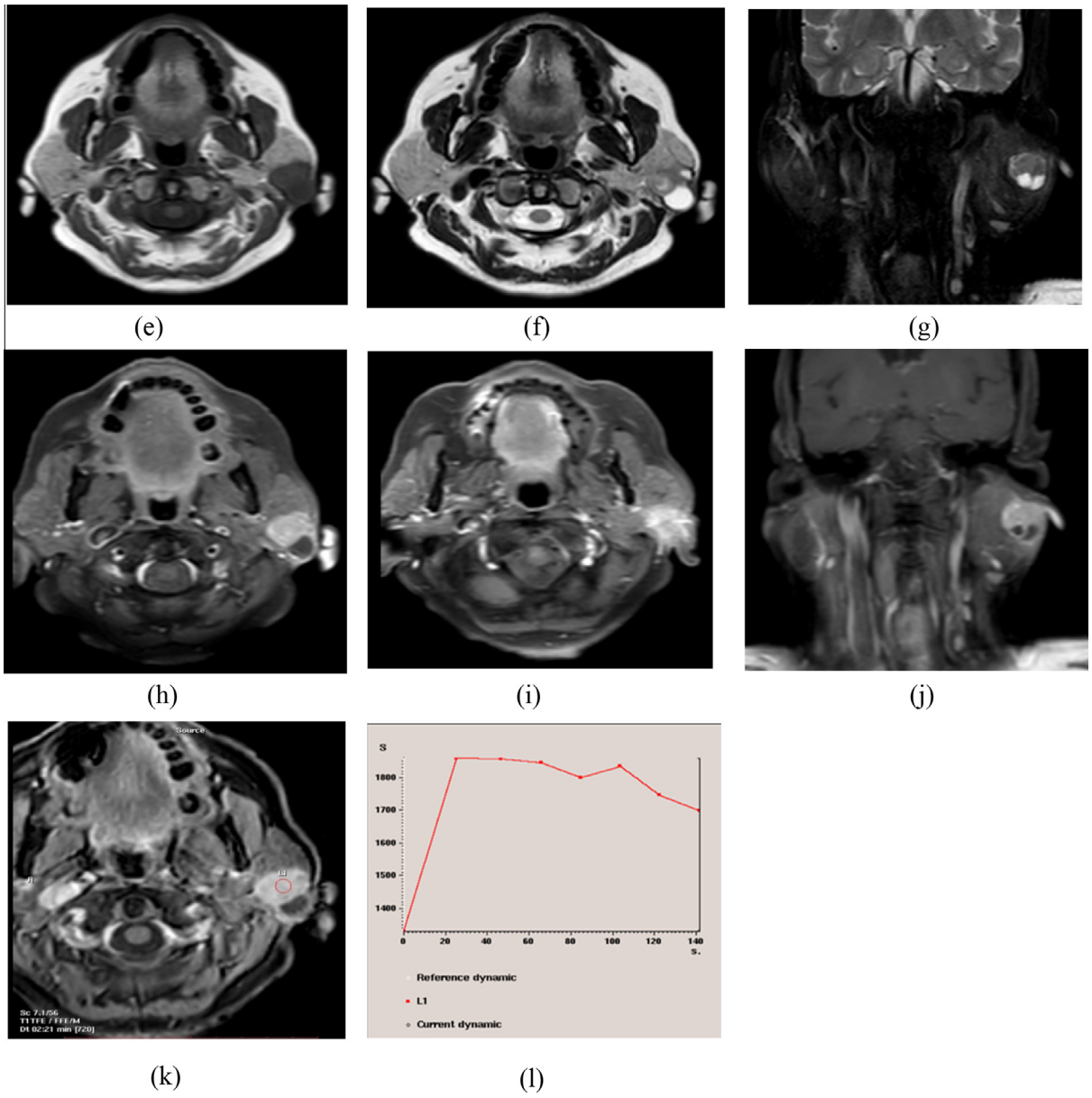

Fig. 4 (*continued*)

and high specificity of 87.5%, positive predictive value of 58%, and high negative predictive value of 89.7%).

Yabuuchi et al. [13] found that the sensitivity, specificity, negative predictive value, positive predictive value, and accuracy of TIC-based tumor differentiation were 91%, 91%, 95%, 83%, and 91% respectively. Our study revealed higher validation study of TIC-based tumor differentiation with high sensitivity, specificity, positive predictive, negative predictive values and accuracy (94.4%, 97.2%, 94.4%, 97.2%, and 96.3% respectively).

Eida et al. [22] found few malignant lesions exhibiting type A curve. This was in accordance with Eissa et al's [9] study in which they found a single malignant case of carcinoma ex-pleomorphic adenoma showing type A curve. Similar results were obtained in our study since we had a case of acinic cell carcinoma that showed type A curve. Again Eida et al. [22] found lesions with type C curve were all malignant. This is contradictory to those by Yabuuchi et al. [23] and Eissa et al. [9] since this curve was exhibited by few pleomorphic adenomas. Also our study revealed Warthin tumor lesions (one on DCE-MRI and two on multiphasic CT) having type C curve.

Eida et al. [22] and Eissa et al. [9] reported that type B curve predominate in Warthin tumors and lymphomas. Our study revealed similar results as regards Warthin tumor but was contradictory as regards lymphoma which exhibited type C curve in our study. This could be supported by a study by Yabuuchi et al. [13] that included 2

cases of lymphoma: one of them showed type C curve and the other showed type B curve.

Ikeda et al. [15] stated that epithelial stroma and lymphoid tissue with small slit like cysts seen in Warthin tumors exhibited early enhancement and a high washout rate (>30%) on dynamic contrast enhanced studies, and accumulation of complicated cysts exhibited early enhancement and low washout ratio (<30%). The average washout ratio of Warthin tumors was significantly higher than that of malignant tumors. This could explain the case of Warthin tumor in our study that showed type C curve.

5. Conclusion

Our study concluded that multiphasic CT with images obtained before contrast, then at 30 s, 90 s, and 5 min after contrast administration with generation of time attenuation curve had comparable high sensitivity, specificity, and accuracy to TIC on DCE-MRI in characterizing different histologic types of parotid gland tumors.

Conflict of interest

The authors declare that there are no conflicts of interest.

References

[1] Nagler RM, Laufer D. Tumors of the major and minor salivary glands: review of 25 years of experience. Anticancer Res 1997;17:701–7.
[2] Pinkston JA, Cole P. Incidence rates of salivary gland tumors: results from a population-based study. Otolaryngol Head Neck Surg 1999;120:834–40.
[3] Magnano M, Gervasio CF, Cravero L, et al. Treatment of malignant neoplasms of the parotid gland. Otolaryngol Head Neck Surg 1999;121:627–32.
[4] Christe A, Waldherr C, Hallett R, et al. Imaging of parotid tumors: typical lesion characteristics in MR imaging improve discrimination between benign and malignant disease. Am J Neuroradiol 2011;32:1202–7.
[5] Habermann CR, Arndt C, Graessner J, et al. Diffusion-weighted echo-planar MR imaging of primary parotid gland tumors: is a prediction of different histologic subtypes possible? J Neuroradiol 2009;30:591–6.
[6] Tatomirovic Z, Skuletic V, Bokun R, et al. Fine needle aspiration cytology in the diagnosis of head and neck masses: accuracy and diagnostic problems. J BUON 2009;14:653–9.
[7] Elagoz S, Gulluoglu M, Yilmazbayhan D, et al. The value of fine-needle aspiration cytology in salivary gland lesions, 1994–2004. ORL J Otorhinolaryngol Relat Spec 2007;69:51–6.
[8] Seethala RR, LiVolsi VA, Baloch ZW. Relative accuracy of fine-needle aspiration and frozen section in the diagnosis of lesions of the parotid gland. Head Neck 2005;27:217–23.
[9] Eissa L, Abou Seif S, El Desooky S, et al. Accuracy assessment of combined diffusion weighed and dynamic gadolinium MR sequences in characterization of salivary gland tumors. Egypt J Radiol Nucl Med 2016;47:127–39.
[10] El Shahat HM, Fahmy HS, Gouhar GK. Diagnostic value of gadolinium-enhanced dynamic MR imaging for parotid gland tumors. Egypt J Radiol Nucl Med 2013;44:203–7.
[11] Yerli H, Aydin E, Coskun M, et al. Dynamic multislice computed tomography findings for parotid gland tumors. J Comput Assist Tomogr 2007;31:309–16.
[12] Jin GQ, Su DK, Xie D, et al. Distinguishing benign from malignant parotid gland tumors: low-dose multi-phasic CT protocol with 5-minute delay. Eur Radiol 2011;21:1692–8.
[13] Yabuuchi H, Fukuya T, Tajima T, et al. Salivary gland tumors: diagnostic value of gadolinium-enhanced dynamic MR imaging with histopathologic correlation. Radiology 2003;226:345–54.
[14] Salama AA, El-Barbary AH, Mlees MA, et al. Value of apparent diffusion coefficient and magnetic resonance spectroscopy in the identification of various pathological subtypes of parotid gland tumors. Egypt J Radiol Nucl Med 2015;46:45–52.
[15] Ikeda M, Motoori K, Hanazawa T, et al. Warthin tumor of the parotid gland: diagnostic value of MR imaging with histopathologic correlation. AJNR 2004;25:1256–62.
[16] Celebi I, Mahmutoglu AS, Ucgul A, et al. Quantitative diffusion-weighted magnetic resonance imaging in the evaluation of parotid gland masses: a study with histopathological correlation. Clin Imaging 2013;37:232–8.
[17] Koyuncu M, Sesen T, Akan H, et al. Comparison of computed tomography and magnetic resonance imaging in the diagnosis of parotid tumors. Otolaryngol Head Neck Surg 2003;129:726–32.
[18] Choi DS, Na DG, Byun HS, et al. Salivary gland tumors: evaluation with two-phase helical CT. Radiology 2000;214:231–6.
[19] Xu ZF, Yong F, Yu T, et al. Different histological subtypes of parotid gland tumors: CT findings and diagnostic strategy. World J Radiol 2013;5:313–20.
[20] Öner AU, Erbaş G, Gültekîn S, et al. Evaluation of parotid gland tumors with multi-phase dynamic helical CT. Gazi Med J 2008;19:6–9.
[21] Chikui T, Obara M, Simonetti AW, et al. The principal of dynamic contrast enhanced MRI, the method of pharmacokinetic analysis, and its application in the head and neck region. Int J Dentistry 2012;2012:1–10.
[22] Eida S, Sumi M, Nakamura T. Multiparametric magnetic resonance imaging for the differentiation between benign and malignant salivary gland tumors. J Magn Reson Imaging 2010;31:673–9.
[23] Yabuuchi H, Matsuo Y, Kamitani T. Parotid gland tumors: can addition of diffusion-weighted MR imaging to dynamic contrast enhanced MR imaging improve diagnostic accuracy in characterization? Radiology 2008;249:909–16.